LOW POWER-ELECTRICAL ISOLATION FOR EKG MONITORING EQUIPMENT

by

David Howard Turkel

Submitted in Partial Fulfillment

of the Requirements for the

Degree of Bachelor of Science

at the

Massachusetts Institute of Technology

June, 1979

Signiture of Author..

Department of Electrical Engineering, 5/ /79

Certified by...

Thesis Supervisor

Accepted by..

Chairman, Departmental Committee on Theses

TABLE OF CONTENTS

LOW-POWER ELECTRICAL ISOLATION FOR EKG MONITORING EQUIPMENT

By

avid Howard Turkel

Supervised by

Professor W. H. Olson

ABSTRACT

The MIT Biomedical Engineering Center for Clinical Instrumentation is currently developing a microprocessor based arrhythmia monitor for ambulatory subjects. In order to provide safe connection of EKG (electrocardiogram) electrodes to patients, electrical isolation of the electrodes from the monitoring equipment is required. Present safety standards mandate a maximum possible leakage of 50 microamperes through the patient's electrodes to the ground plane for battery operated devices. MIT's portable monitor has the additional constraints of:

1) less than 50 mW total power dissipation for the isolated amplifier
2) a transfer linearity approaching .1%
3) frequency response of .02 Hz to 100 Hz
4) small physical dimensions
5) available supplies are ± 5 volt and 12 volt.

To meet these requirements several isolation methods were investigated. After opto-isolators were chosen as the most desirable signal isolation device, calculations were made to determine the opto-isolator's power requirements when operated using amplitude modulation, phase modulation, and frequency modulation. Low-power circuits for these modulation schemes were designed, constructed, and tested. The amplitude modulation circuit was found to be the closest to the design specifications. An amplitude modulation circuit for an isolated EKG preamplifier was designed for the prototype arrhythmia monitor.

As microprocessors are allowing the creation of portable medical instrumentation, a need has arisen for certain low-power-consumption circuitry. One such circuit is required to provide electrical isolation of EKG (electrocardiogram) electrodes between the patient and the equipment. This isolation might not only protect the patient from the possibility of electric shock, but would protect the portable EKG equipment from damage if high-voltage defibrillation pulses are applied to the patient.

In 1971 Ralph Nader and Carl Walter claimed that 1200 Americans were electrocuted each year during routine diagnostic and therapeutic procedures.[1] Although this figure would be hard to validate, this type of claim helped bring attention to research on human vulnerability to electric shock. This research has indicated that patients are particularly susceptible to shock when devices are placed into or near the heart or if electrodes outside the body produce a current path through the heart.[2] It was reported that fibrillation in dogs can be induced with currents as low as 20 microamperes and the sparse data for humans indicated that currents ranging from 80 to 600 microamperes can cause fibrillation.

When a portable EKG monitor is battery operated, one might suspect that the low voltage batteries or power supplies would be unable to cause electric shock. However, if the equipment is to be connected to line-powered computers for testing or data transfer, it would have to meet the accepted safety standards for line-powered hospital equipment. Considering that skin resistance[3] can vary from about 1 megohm/cm.^{2} to 15 kohm/cm.^{2} it appears that a large voltage is required to cause significant current density through the heart. Nevertheless, the widely accepted NFPA safety codes for biomedical equipment require that no more than 50 microamperes be present at the external patient electrodes.[4]

Examination of the schematics of several commercially available line-powered EKG monitors yielded several methods used to meet the NFPA codes and also to protect the equipment from defibrillation spikes. All of the designs included surge-suppression, gas-filled discharge tubes (with a typical breakdown at 90 volts) across the patient electrodes to protect circuitry if large defibrillation pulses are applied to the patient. Defibrillation devices often produce pulses with a magnitude of several thousand volts.

Isolation of the EKG signal was performed through a more diverse set of methods. Three of the circuits examined used transformers for signal isolation. In each of these cases, the amplified and filtered EKG signal was used to create an amplitude modulated (AM) signal by using either JFET's or CMOS analog switches to multiply the EKG signal by a high-frequency square-wave carrier. One of the monitors used an opto-isolator (matched LED and phototransistor in one package) and used a discrete VCO (Voltage Controlled Oscillator) to create a frequency modulated (FM) signal to cross the optical isolation. A "linear-series" phase locked loop (PLL) was used to demodulate the signal from the opto-isolator.

Burr-Brown manufactures "Optically Coupled Linear Isolation Amplifier Modules." Despite the excellent linearity and isolation capabilities of these modules, they require far too much power for our portable equipment operation as is the case with each of the existing commercial circuits. The Burr-Brown modules claimed a linearity (defined as deviation from a best straight line) of .05% and isolation up to 5000 volts peak. Nevertheless, the minimum power requirement of almost 100 milliwatts and price (over $40/module) made them unsuitable for our low-power application. Meeting the stringent power-dissipation constraint for this project lead to the rejection of several other designs.

In addition to signal isolation, power-isolation is required to meet the NFPA codes. Power isolation was performed, in these commercially available devices, with transformer based DC-DC converters buit to have a low coupling capacitance, However, isolation transformers are able to pass spikes in both directions and are usually larger than desired for a very limited-size portable device. A more total isolation, and, perhaps, more patient and circuitry protection would be provided by using a separate battery power supply for the front-end circuitry and the patient's side of the signal isolation

As a result of smaller size and greater isolation capability, opto-isolators seem more desirable than coils for use with small portable equipment. However, the opto-isolators currently available require significant currents to power the LED (the transmitting device in isolator) and typical operating currents of greater than 15 mA is required for some optocouplers[5](e.g. 6N136, HP:HCPL2502, etc.). Fortunately a line of low input current opto-couplers have recently become available (including 6N139, 4N46,6N140,HP:HCPL 2731) which have typical specified input currents of .5 mA. The only obvious advantage of the higher current devices is a slightly higher capability for high-speed data transfer.

After a search of available opto-isolators, the HP 6N139 was chosen as a trade-off between bandwidth and power consumption. It allows low-power use for analog modulation schemes and also has a reasonable, high data transfer rate when digital modulation schemes are used (up to 1 MHz). Although some data was given on the diode characteristics of this device (the LED half), I decided to check the V-I characteristics so that estimates of power-dissipation could be made for different modulation schemes. A plot of this data (table 1) on a semi-log scale resulted in a straight line as is expected for a diode (see graph 1).

As a result of the exponential nature of the diode V-I characteristics, the approximation

$$I_F = A\, e^{b\, V}$$

where V = Forward voltage across diode
I_F = Current through diode

for suitable values of A and b.

In semi-log terms $I_F = A\, e^{b\, V}$ or $y = A\, e^{b\, x}$ is represented by the line

$$\ln(y) = \ln(A) + bx \quad \text{or} \quad \ln(I_F) = \ln(A) + b\, V_d\ .$$

Applying a least-squares regression to this line, the values for A and b were determined for the data in table 1;

$A = 7.5 \times 10^{-12}$
$b = 17.8$

when V_d is in volts
and I_F is in mA.

Using this exponential approximation one observes an excellent fit to the actual data (see table 2). Now, with this approximation it is possible to attempt theoretical derivations for power required by this isolation device when when different modulation schemes are used. However, these derivations are constrained to a limited bandwidth where the device's capacitive effects are insignificant (typically where operating frequency is less than 300 kHz).

Modulation Methods

Amplitude modulation is one of the simpler methods to transmit the EKG signal across the isolation. As already stated, it was used in three of the examined commercially available EKG monitor isolation circuits. In each case a coil was used as the isolation device and a carrier of several kiloHertz (10 kHz to lo2 kHz for those examined) was used to modulate the slowly varying EKG signal which is considered to vary from .05 Hz to 200 Hz. For this scheme, modulation is performed by multiplying the input signal by a carrier signal as shown in figure 1. The carrier frequency is usually chosen to allow accurate demodulation and to conform to device or efficiency constraints. Typically, demodulation is performed in one of two ways. First, it is possible to low-pass-filter the modulated signal. Second, if one has a way to know the phase of the carrier (on both sides of isolation) and coils are used with an offset EKG signal, quadriture multiplicati may be used as shown in figure 2.

If the support circuitry has negligible power consumption, the total isolation power required will be about the same as the power dissipation in the opto-isolator LED. This power can be approximated by considering the average power per cycle at different frequencies. Consider the signal shown in figure 3. The average power as a function of frequency is given by

$$\overline{P} = f\,D \int_0^{1/f} V_d(t)\; I_d(t)\; dt$$

where f is frequency

D is duty-cycle fraction

$V_d(t)$ is diode voltage

$I_d(t)$ is diode current

or more specifically:

$$\overline{P} = f\,D \int_0^{1/f} V_b\;(1 + X \sin(2\pi ft)\; A e^{V_b\, b\,(1 + X \sin(2\pi ft))}\; dt$$

where V_b is the DC bias of the carrier (see figure 3)

X is size of voltage variation around bias

A and b as defined on page 6

Now, for the special case where D = 1 (DC carrier)

and for $A = 7.5 \times 10^{-12}$ and b = 17.8 as found for the 6N139 opto-isolator LED,

with V_b = 1.3 volt (for example -- used in a test circuit to be described)

X = variation magnitude = .050 volt

we obtain the result that $\overline{P}$ is about .15 mW at .2 Hz, 10 Hz, and 100 Hz but $\overline{P}$ decreases with increasing frequency. Additionally, this constancy of power over frequncy is related to X. For larger X the power consumed rapidly increases. MACSYMA, a Navy supported system/program was used to solve these integrals with a numerical approximation.

An AM optical isolation with a DC carrier signal (and bias) allows the use of simple isolation support circuitry. One early attempt at this type of analog isolation is documented in "Modulated Light Transmission for Electrical Isolation in a Multichannel Physiological Monitering System" as published in Aerospace Medicine[6]. The authors propose that a circuit of the form shown in figure 4, using a non-monolithic LED and photodiode, gives useable linearity. Their circuit dissipated over 300 mW as they designed it. For our applications a lower current is required when driving the LED so that a low-power op-amp from the input stage may be used to drive the LED directly. To minimize power, we should operate the opto-isolator at the minimum allowable V_d level and allow for only enough signal variation to meet the linearity requirements. For use with a 6N139 it seems that $V_d = 1.30$ volts is a reasonable quiescent operating voltage. A 50 mV voltage variation around this point will lead to a doubling and halving of I_d and thus may provide sufficient output noise immunity with acceptable transfer linearity. This circuit is shown in figure 5.

A circuit similar to the one in figure 5 was constructed in order to measure power required for isolation. To minimize quiescent power requirements a single transistor, common-emitter stage was used to drive the optical isolator. The test circuit is shown in figure 6 and its associated transfer function (from data) is provided as graph 2.

Theory / Analysis of circuit design: AM

To operate so $V_d = 1.3$ volts, a current of about .1 mA will be required (see graph 1). Modeling the diode as a resistor for small voltage deviations, $R_{eff} = V_d / I_d = 1.3\text{volt}/ .1\text{ mA} \approx 13$ Kohm. As a result of this large effective R, we can use $R_3 = 100$ ohm and not strongly affect the voltage presented to the diode. This 100 ohm resistor will act as a current-limiting resistor to protect the diode from currents greater than $V_{s1}/100$

or I_d = 50 mA in this case. Since R_{eff} = 13 Kohm, the bias resistance, R_b (R_1 // R_2), should be about 10 R_e or about 130 Kohm. Also, we want V_{b1} = V_{dq} + V_{be} or V_{b1} = 1.3 + .6 = 2. volts in this case. So

$$R_1 = R_b \frac{V_{s1}}{V_b} \qquad \text{and } R_2 = \frac{R_1 R_b}{R_1 - R_b}$$

In order to have adequate low-frequency response for this simple circuit a large coupling capacitor is required. However, this can be avoided if the previous stage provides a constant offset of V_{b1} as already mentioned. Otherwise, for f_L = .2 Hz, $\tau_{sc}\Big|_{capacitor}$ = 5 ·2π . The representative circuit and equation for τ_{sc} is shown in figure 7. For the parameters of this circuit (R_b = 130 KΩ, R_{source} = 27Ω, R_e = 13 KΩ) and a transistor with a β = 100, we calculate C_1 = 2π5/(130KΩ // 100(130KΩ)) = 240 μF. As large capacitors affect overload (or saturation recovery) time, and take up space, they should be avoided and direct coupling is therfore preferred.

The circuit that was constructed used C_1= 100 μF and slightly less optimal values for R_b. Nevertheless, it performed linearly over a usable voltage range (over 100 mV), Data was taken on AC performance and showed that I_{CQ} = 2 mA and I_c (100 HZ) = 1.7 mA. This power dissipation of P=VI= (5 v.)(2 mA) = 10 milliwatts for the isolated side of the circuit and a dissipation of V_{s2} / 10KΩ = 2.5 milliwatts for the phototransistor side. A linear regression program was applied to the data chart(table 3) which gave a correlation coeficient of greater than 1.0000 - 1.3 x 10^{-4}. At lower frequencies the slope of V_0/V_i changes by a few percent even though linearity was maintained (see graph 3). This may have resulted from either inadequate test accuracy, a constant test error, or insufficiently large coupling capacitor.

Although this isolation driver might work in a will shielded environment, it does not have differential inputs and therefore a low CMRR results. This will not be a problem if it is preceded by an instrumentation amplifier with differential input and assuming that there is no noise on the V_{s1} supply.

Of the commercially available equipment examined one used frequency modulated (FM) isolation. This modulation was done by feeding the preconditioned EKG signal to a discrete multivibrator which acted as a VCO. After optical isolation, the signal was recovered by demodulation with a phase locked loop and a two-pole active filter.

This modulation scheme may be used with either coils or fast optical devices. It is designed so that the modulator will create a linear relationship between ouput pulse frequency and input voltage. Demodulation requires an oscillator operating at f_o (approximately the mean frequency or "center frequency") from which differences in phase with $f_{modulated}$ is found. This phase difference is low-pass-filtered and fed-back to the VCO to adjust its operating frequency in a direction to match the $f_{modulated}$. The low-pass-filtered voltage that is fed to the VCO is linearly related to the input voltage.

The power dissipation in the opto-isolator LED, for one cycle of modulated signal is easily estimated. Since there will be some mean frequency of operation, f_o, with a symmetric variation around that frequency so that the average power is described by

$$\overline{P} = V_p\, I_d(V_p)\, D$$

where V_p is voltage of frequency modulated pulse at LED

$I_d(V_p)$ is the diode current for V_p at the LED

D is duty-cycle fraction

As a relevant example, for $V_p = 1.4$ volt

$I_d(V_p) = .5$ mA (see graph 1)

$D = .50$

the resulting power dissipation $\overline{P} = (1.4)(.5)(.5) = .35$ milliwatts. With the present diode model which does not include capacitance, the result is frequency independent. This calculation assumes the f_0 is sufficiently low so that capacitive losses in the diode are negligible.

Today's CMOS and linear technology has provided several easy to use PLL chips useful in both modulation and demodulation. Although most of the "linear" devices (e.g. the 560 series) provided well under 1% distortion[7] (.2% typical according to Signetics "Analog Data Manual") their quiescent operating powers are, perhaps, excessive for the low-power conditions required here. A SE 567 has the lowest I_q of the series[8] with 7 mA at $\pm$ 5 volts, or a quiescent power drain of 70 milliwatts. Nevertheless, the ease of use of these devices makes them useful for less power-stringent applications. A CMOS CD4046B PLL is rated at a dynamic power consumption of typically 70 microwatts with f_0 = 10 KHz. Also, Cmos voltage requirements allow a wide range of operation[9].

The low-pass filter shown in figure 8, a diagram of a PLL FM demodulator, is an important part of the PLL design. The characteristics of this filter will determine the capture range and lock range. If too low a cutoff is used, the PLL will never lock to ω_i (see figure 8). Under some conditions the loop acts like a second order feedback system and can have damping factors less than $\sqrt{2}$ / 2 leading to overshoot of the locking frequency by the PLL. To test the utility of the CD4046 in low-power isolation applications the circuit in figure 9 was constructed.

For the configuration shown in figure 9, calculations were performed to determine R_1 and R_2 to give the VCO an oscillation range of 10 kHz to 20 kHz. As can be seen, the circuit was designed with a CMOS-based monostable to allow variation of the duty-cycle seen by the LED of the opto-isolator. Data for the DC transfer characteristics of this isolation circuit was collected and is given in table 4. A plot of these data (graph 3) shows that, over the entire test range, linearity was not better than 2%. However, in the region where V_o was between 3.5 and 6. volts, the transfer characteristics were very linear with a maximum deviation of less than .3% . The AC data showed a constant transfer function at very low frequencies and a -3db point at 200 Hz. At 100 Hz the V_o/V_i value was down about 5 % from its very low frequency value.

The current required by the isolated half of the circuit (VCO, monostable, transistor driver) was 19 mA at 10 volts and about .5 mA at 10 volts was required by the demodulator side. Thus, for a 50% duty-cycle, the total isolation power required was about 25 milliwatts. Although this power demand exceeds what might be expected for this type of CMOS circuitry, it is within a range which makes it suitable for use in low-power portable equipment.

For phase modulation the phase of the modulated signal is varied from that of a shared reference signal. The phase difference is proportional to the modulating voltage as shown in figure 10. Modulation can easily be performed with a PLL as shown[10] in figure 11. The shared carrier can be a preconditioned square wave extracted from an isolation-transformer used to power the circuit, or it can be a signal passed over a second opto-isolator. Demodulation can crudely be achieved by low-pass filtering a signal found by applying an exclusive-or to the carrier reference signal and the phase-shifted carrier.[11]

Power consumption for the phase-modulated circuit should be very close to that for the FM circuit. Assuming the reference is passed through a power-isolation transformer, the power dissipated in the single opto-isolator follows the same formula as used for the FM circuit. If a second opto-isolator is used to transmit the reference signal, the power requirement would increase significantly although the final power requirement should be less than two times the requirement for the FM circuit.

The test circuit shown in figure 13 was constructed and transfer-characteristic data is provided in table 5. A graph of this function is shown in graph 4, indicating a smaller linear operating range than found in the FM circuit. Additionally, the linearity was slightly worse, as the maximum deviation from the line of best fit was about .4% . For some reason the circuit showed roll-off for EKG frequencies above 100 Hz and had a -3db point at 125 Hz. Power-consumption was slightly higher than for the FM circuit, as 30 milliwatts were dissipated by the transmitting side and

2 milliwatts by the receiving side.

Comparison of Methods

In figure 14 a comparative chart of the three isolation circuits is provided. In this chart one may notice that the AM circuit required less than half the power needed by the phase modulation or frequncy modulation circuit. Additionally, it was the physically smallest circuit and only required one data path, whereas the phase modulation circuit required two (one for the reference signal and one for the phase-shifted signal). The FM circuit showed a linearity of .2% and would probably be less sensitive to power-supply voltage variation than the AM circuit. The sensitivity of the AM circuit to the power-supply is based on the fact that the opto-isolator's linearity is strongly a function of quiescent operating voltage.

As the AM circuit was small, simple, required the least power, with excellent linearity, amplitude modulation was used in the actual EKG preamplifier and isolation circuit.

The final design used a modified version of an EKG front-end preamplifier described in a letter from PhysioControl Corporation[12] but with an op-amp driven, analog, small-variation amplitude modulation over an opto-isolator. The total power requirement for this circuit, with the opto-isolator, was well under 10 milliwatts with a ± 5 volt isolated supply.

LIST OF FIGURES

Footnotes

[1]W.H. Olson, "Electrical Safety," in Medical Instrumentation. ed. John G. Webster (Boston :Houghten Mifflen, 1978), p. 673-675.

[2]Ibid., p. 675.

[3]Ibid., p. 679.

[4]Ibid., p. 675

[5]Hewlett Packard 1978 Optoelectronics designers catalog, (Hewlett Packard, 1978), p. 156.

[6]Donald G. Forgays et. al. "Modulated Light Transmission for Electrical Isolation in a Multichannel Physiological Monitering System," Aerospace Medicine, (January, 1973).

[7]Signetics Analog Data Manual, (Sunyvale, Signetics, 1977), p. 596.

[8]Ibid., p. 596.

[9]Motorola Semiconductor Products Vol. 5/B CMOS Semicinductor Data Library. (Motorola, 1977), p. 5-115.

[10]Ibid., p. 847.

[11]Don Lancaster, CMOS Cookbook, (Indianapolis, Howard W. Sams, 1977), p. 255.

[12] Personal Communication with PhysioControl, November,1978.

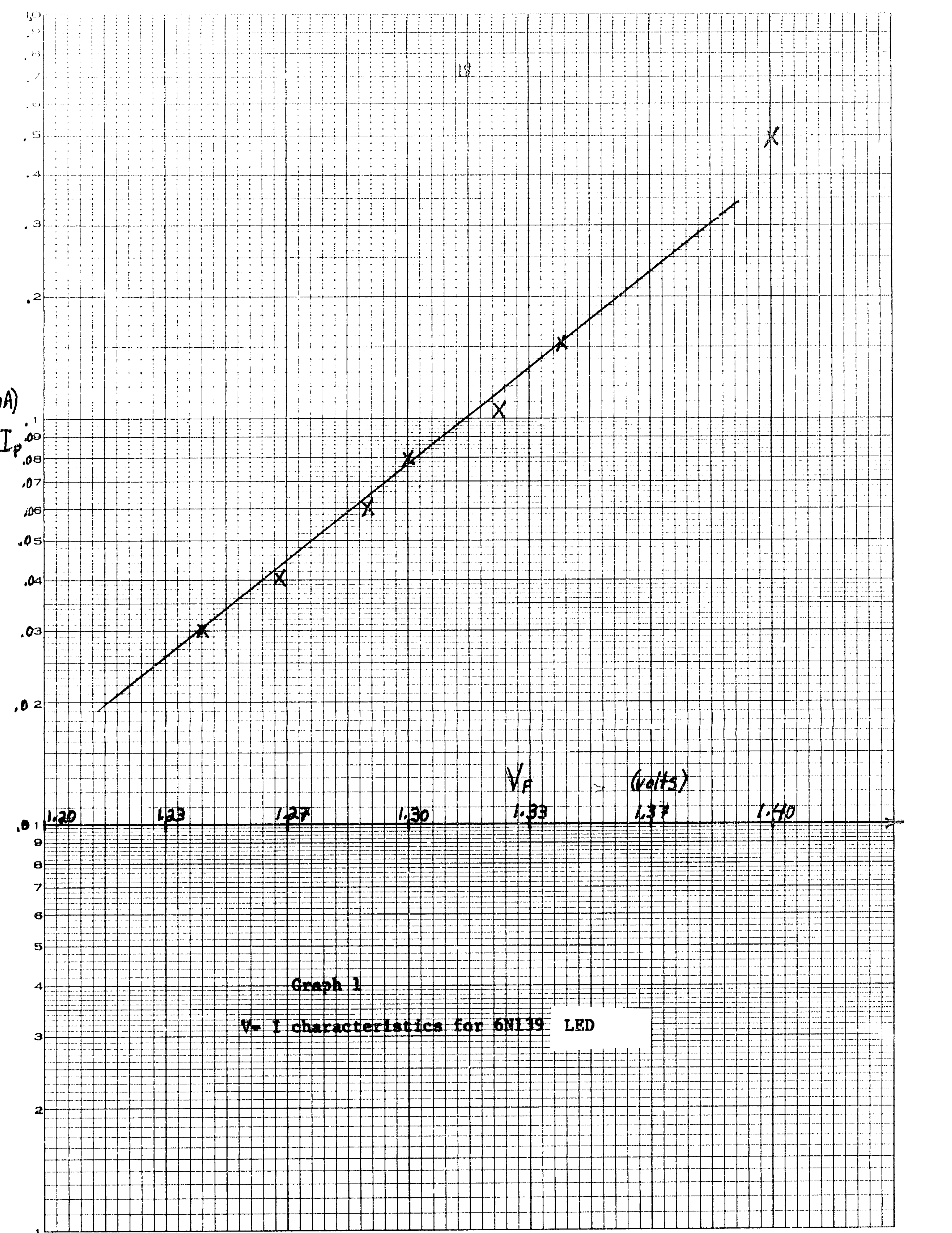

Graph 1

V- I characteristics for 6N139 LED

AM transfer characteristic

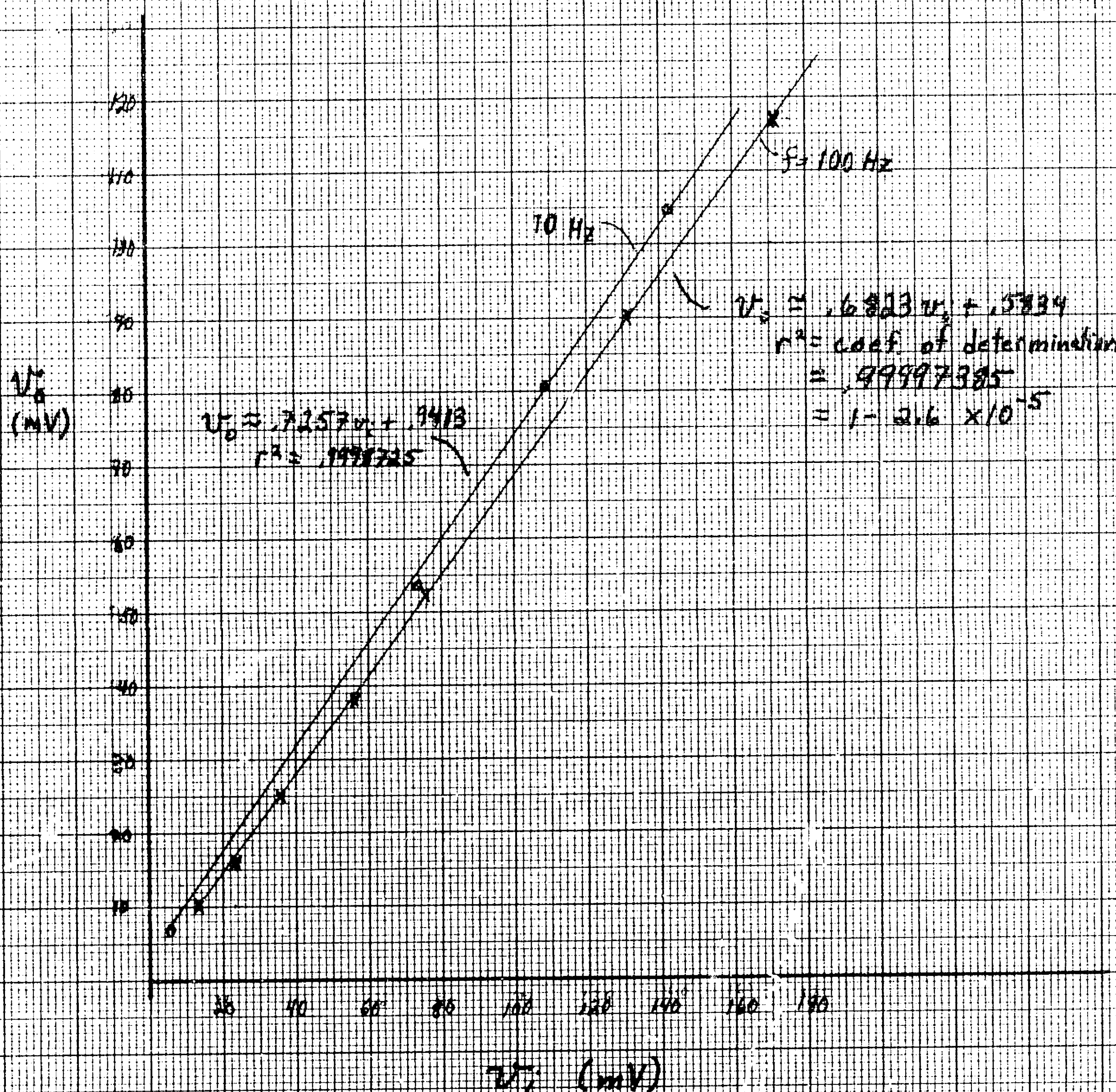

Graph 2

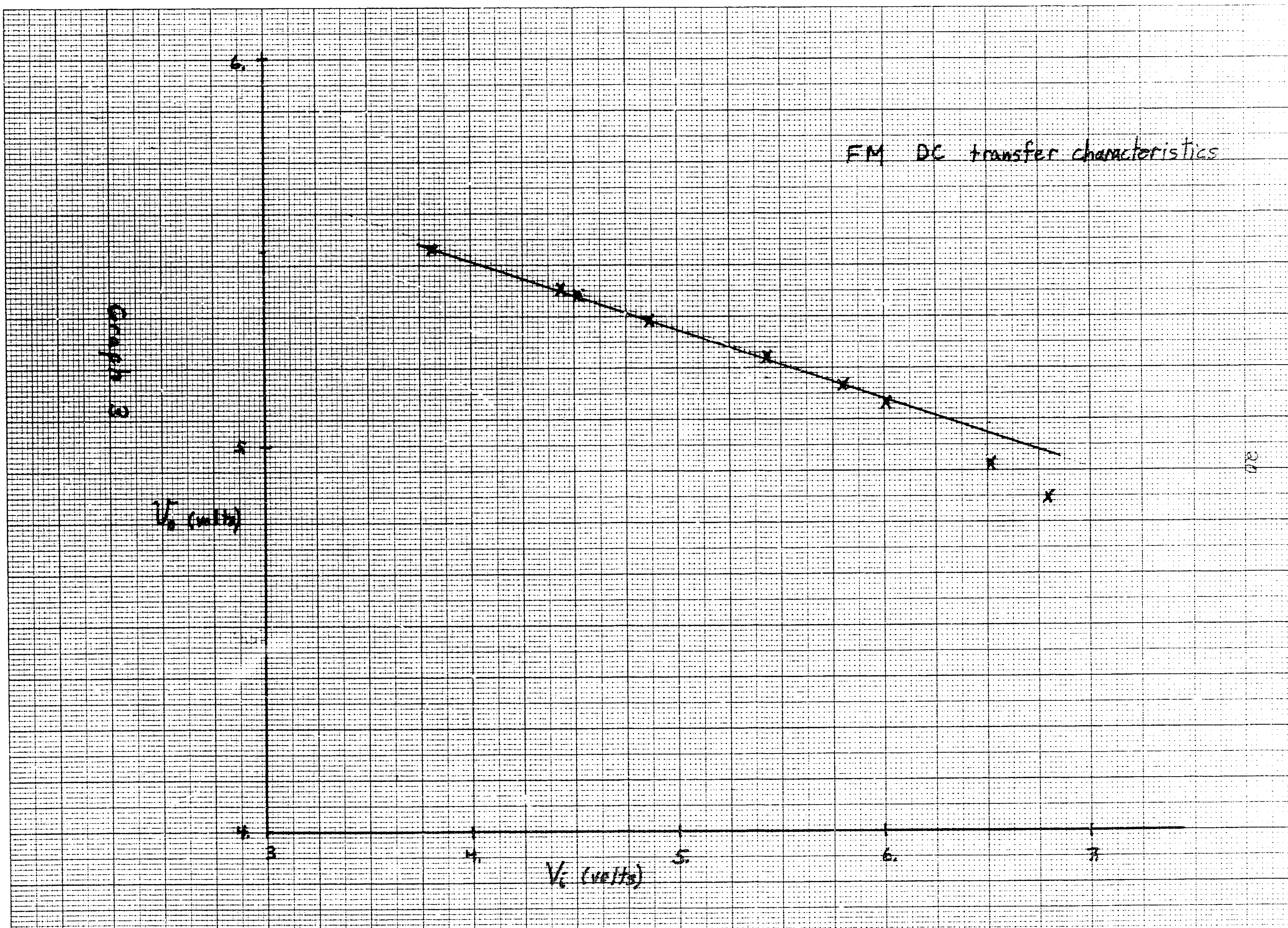

FM DC transfer characteristics
Graph 3
V_o (volts)
V_i (volts)
6.
5
4.
3
4.
5.
6.
7

FM

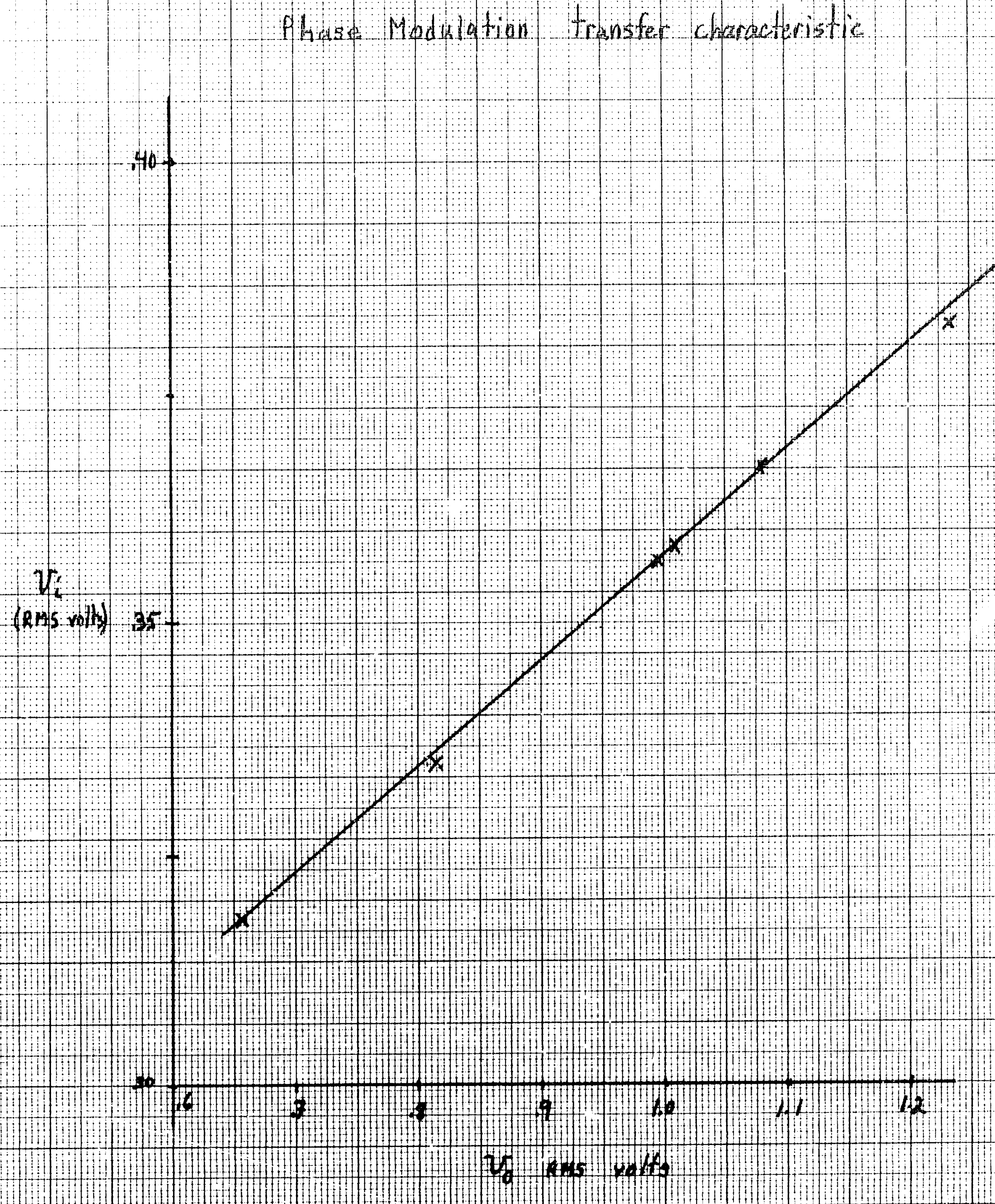

Phase Modulation transfer characteristic
.40
V_i
(RMS volts)
.35
.30
.6
.7
.8
.9
1.0
1.1
1.2
V_o RMS volts

Graph 4

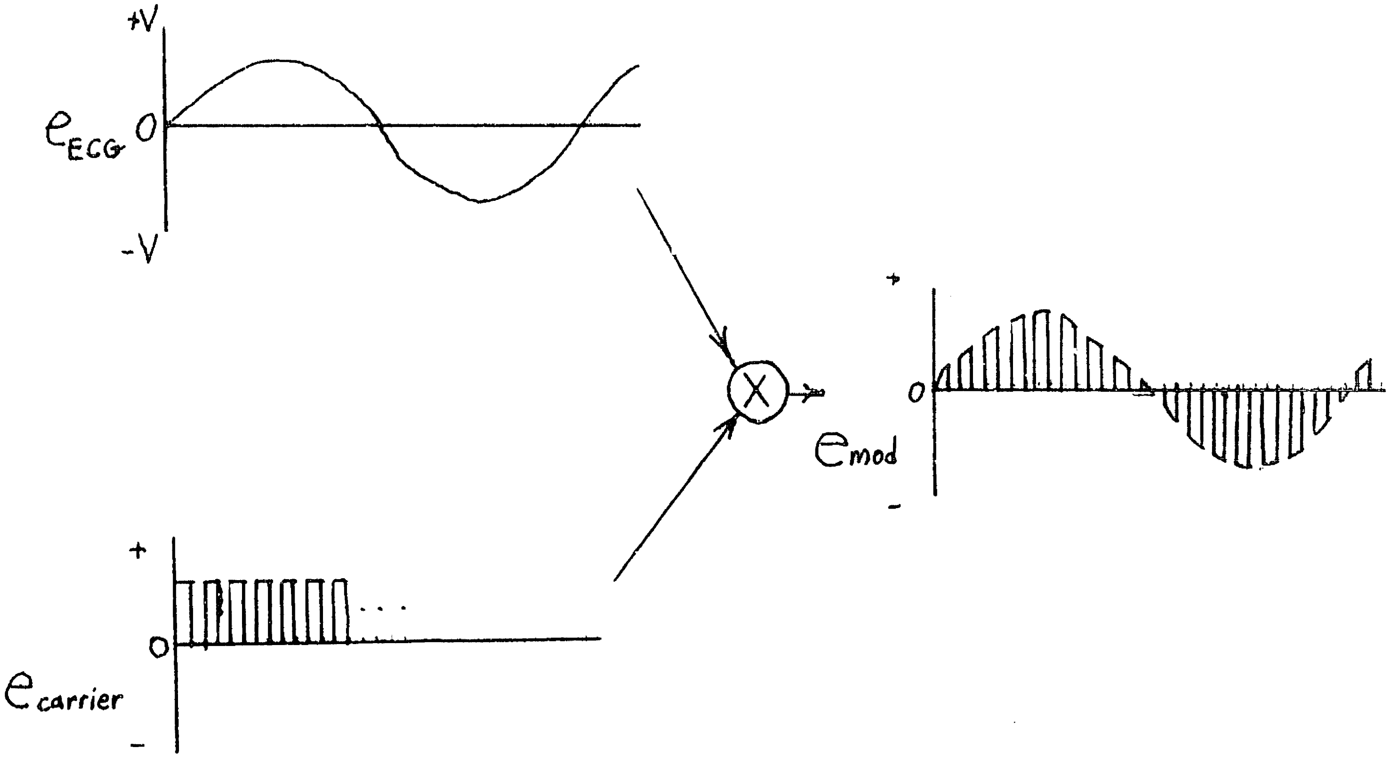

figure 1

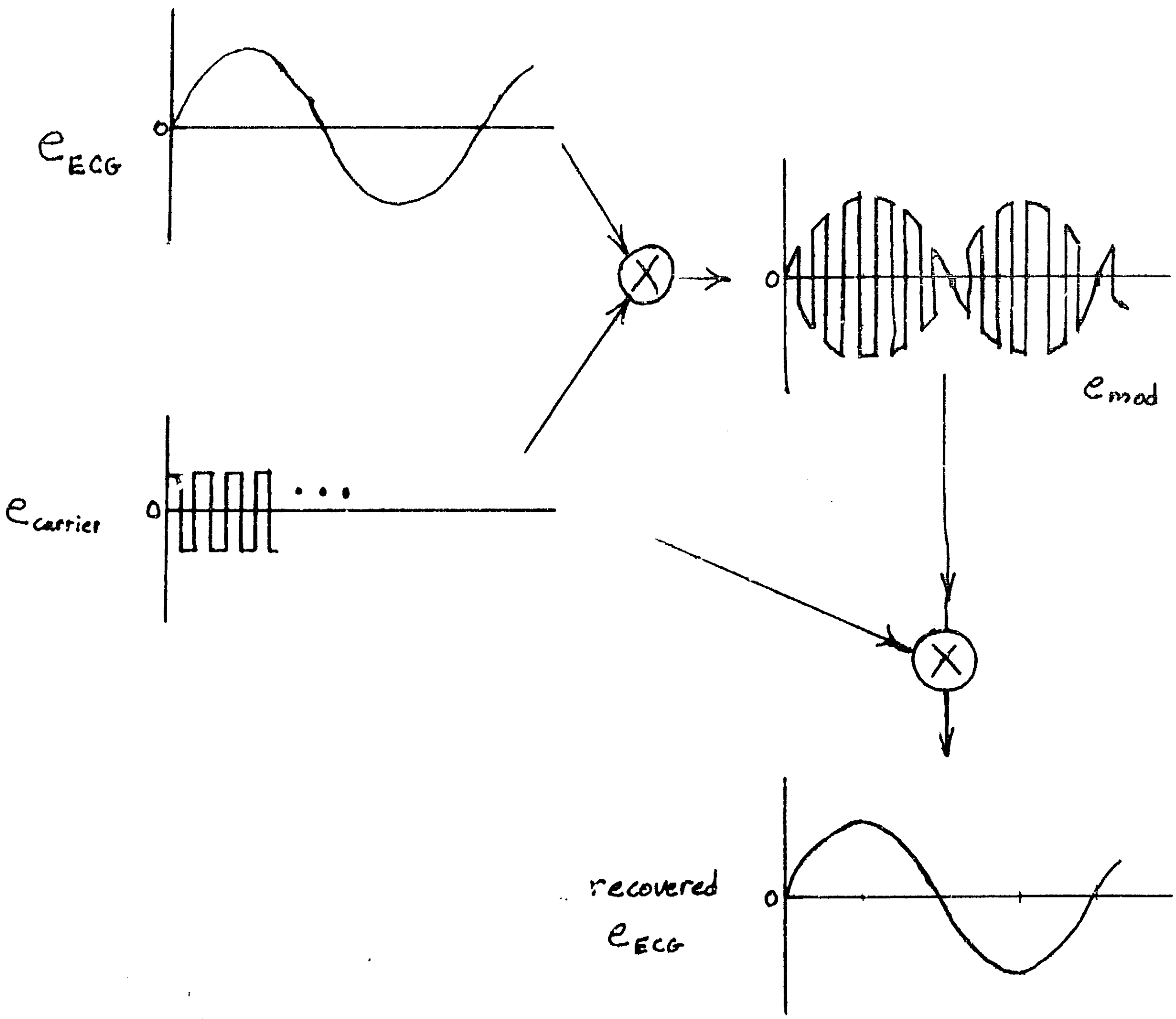

figure 2

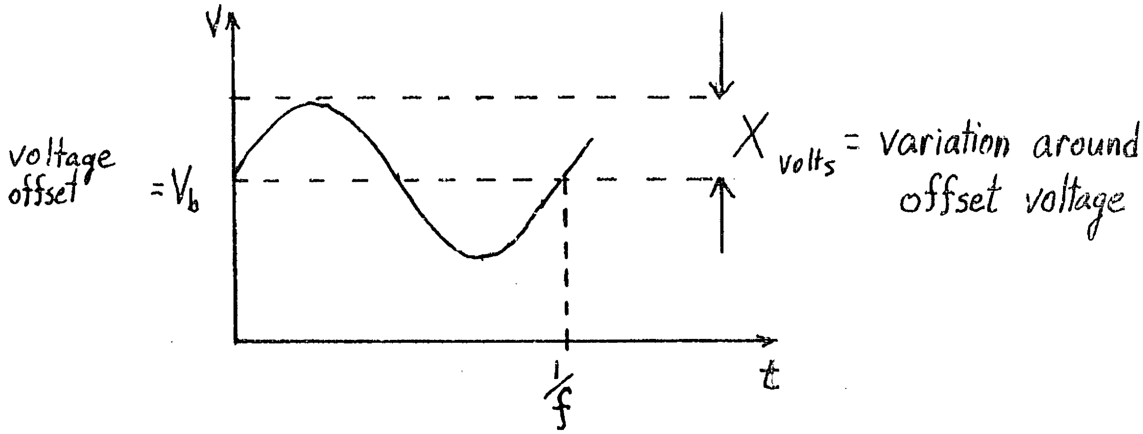

V
voltage offset
$= V_b$
X_{volts} = variation around offset voltage
1/f
t

figure 3

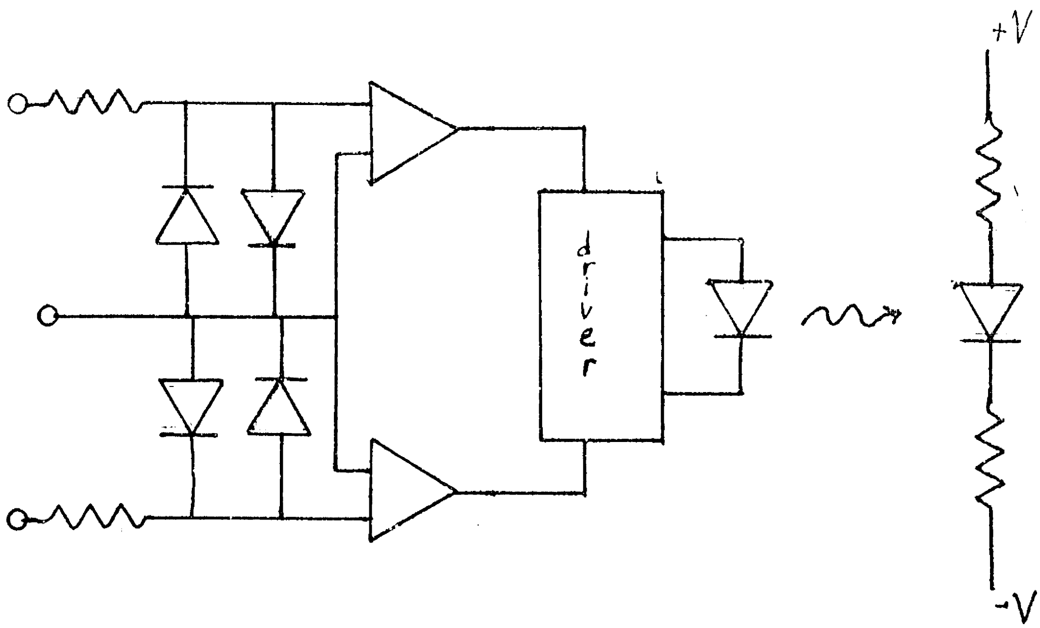

figure 4

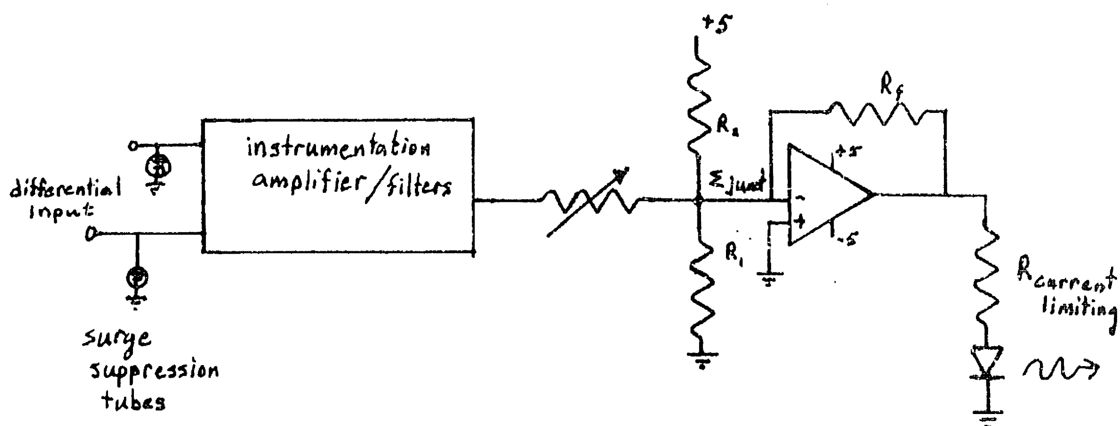

differential input
surge suppression tubes
instrumentation amplifier/filters
+5
R_2
R_f
+5
Σ_{junct}
-
+
-5
R_1
$R_{current}$ limiting

figure 5

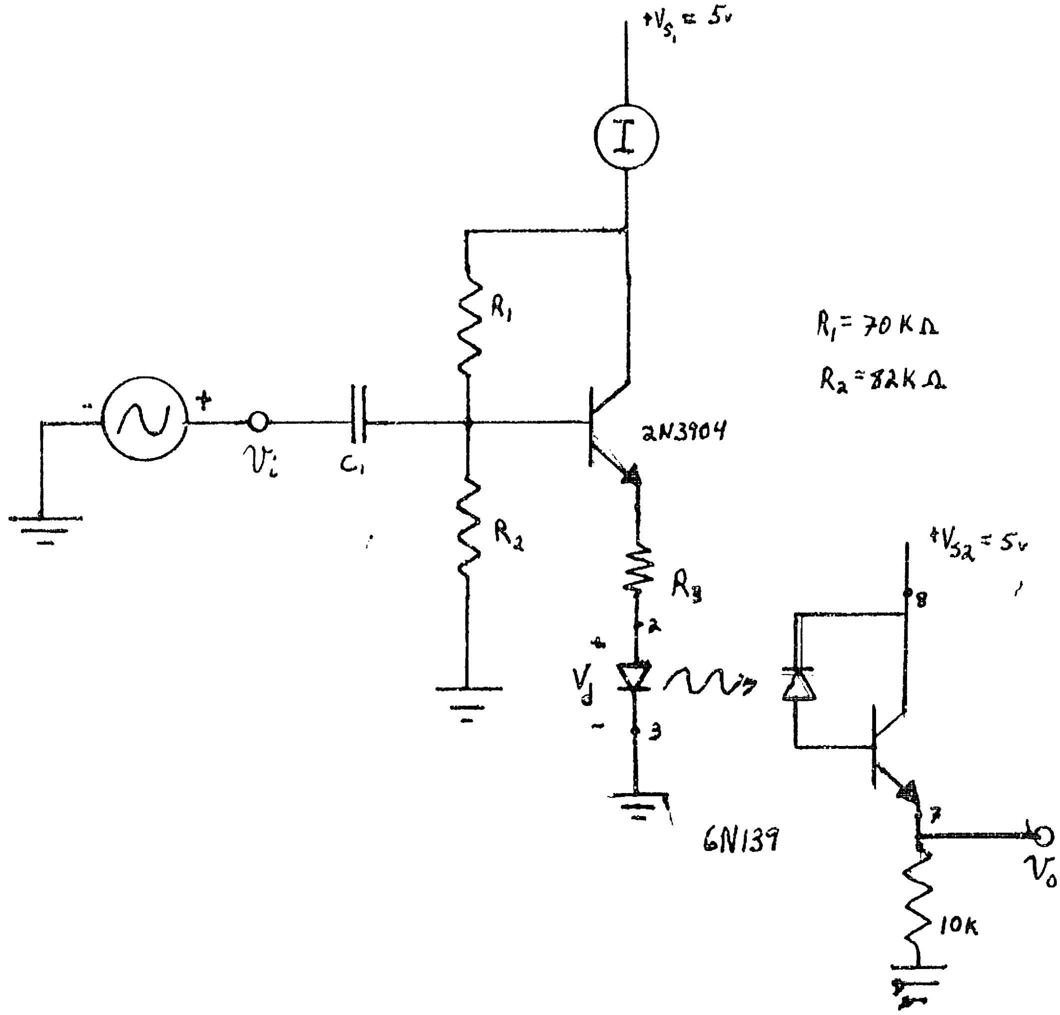

$+V_{S_1} = 5v$
I
R_1
$R_1 = 70 K\Omega$
$R_2 = 82 K\Omega$
+
v_i
C_1
2N3904
R_2
R_3
$+V_{S2} = 5v$
8
2
+
V_d
-
3
6N139
7
V_o
10K

figure 6

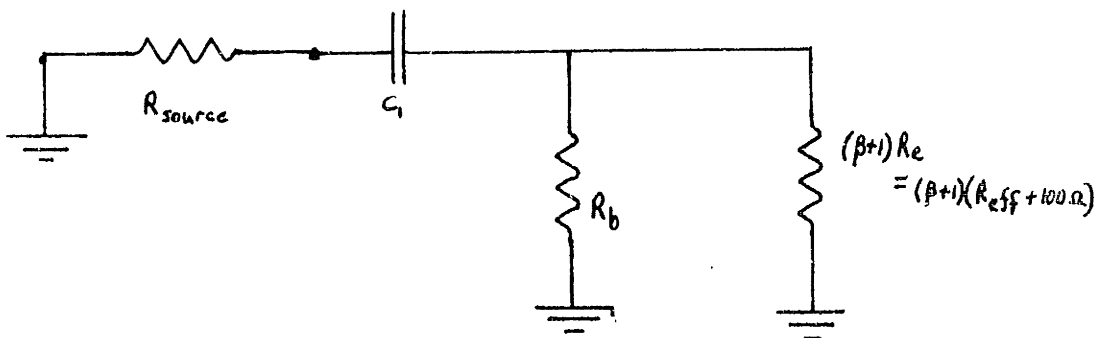

$$\tau_{sc} = C_1 \left(R_s + R_b // (\beta+1) R_e \right)$$

figure 7

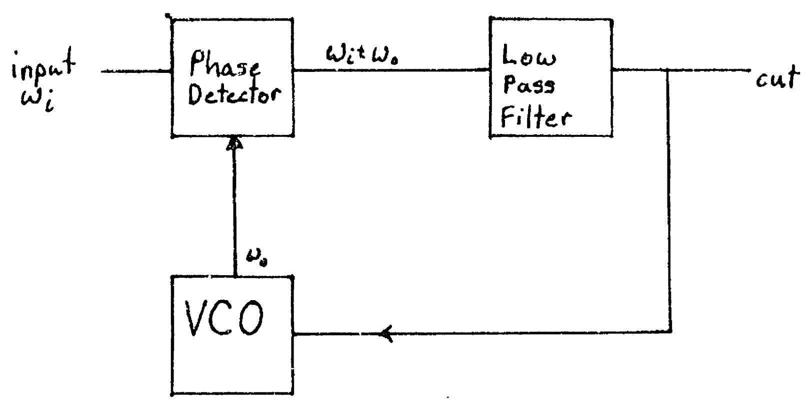

(based on diagram in
Signetics "Analog Data Manual"
Section 26, 1977)

figure 8

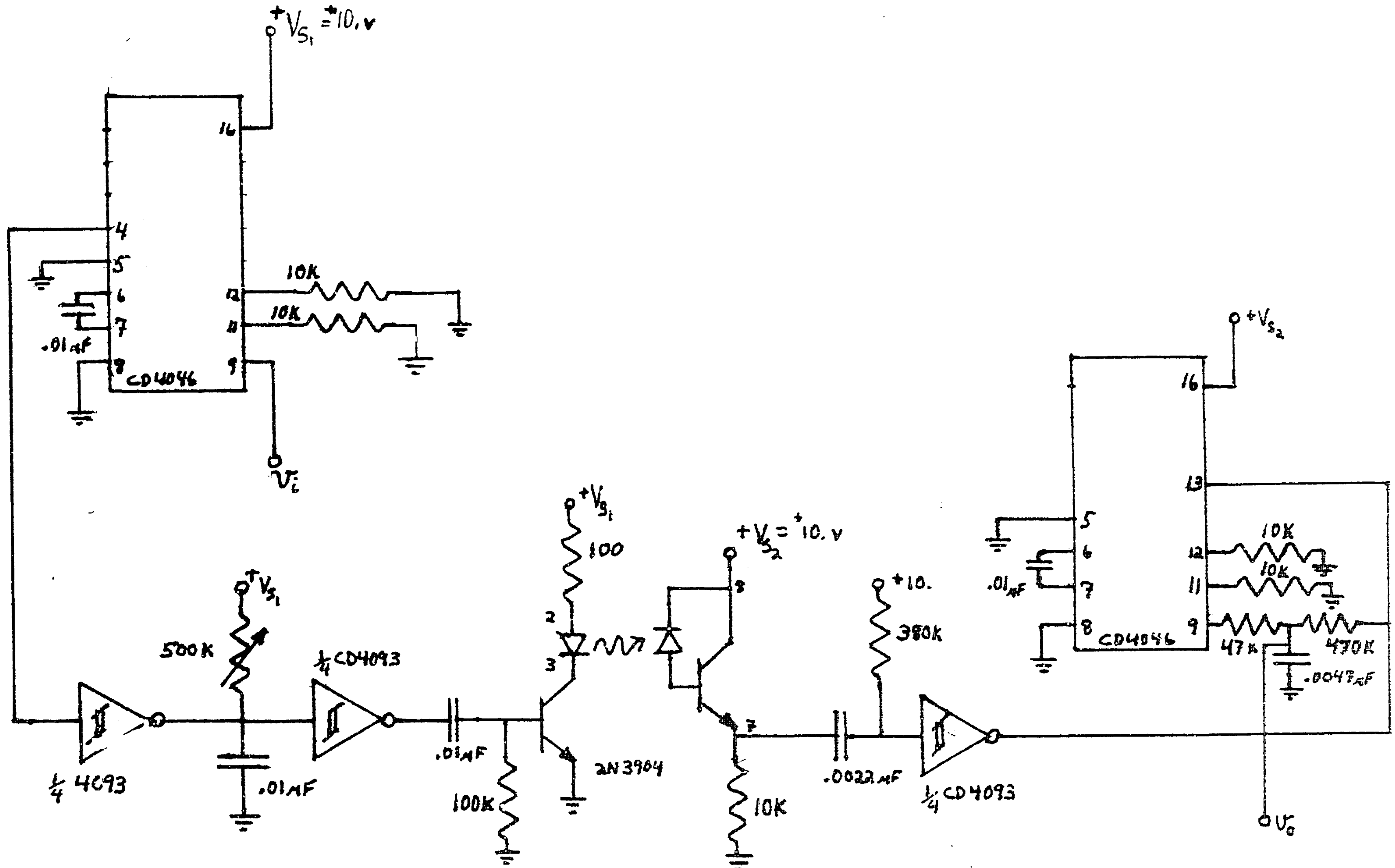
+Vs1 = +10.v
16
4
5
6
7
8
12
11
9
10K
10K
.01μF
CD4046
Vi
+Vs1
100
2
3
+Vs2 = +10.v
+Vs1
500K
1/4 CD4093
1/4 4093
.01μF
.01μF
100K
2N3904
+10.
380K
.0022μF
10K
1/4 CD4093
+Vs2
16
13
5
6
7
8
12
11
9
10K
10K
.01μF
CD4046
47K
470K
.0047μF
Vo

figure 9

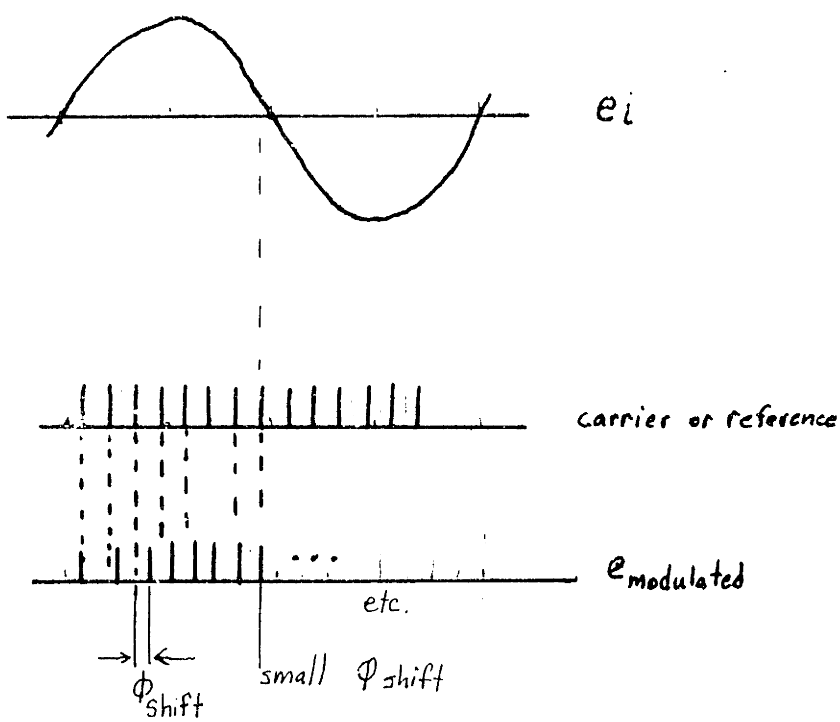

ei
carrier or reference
emodulated
etc.
small φ shift
φshift

figure 10

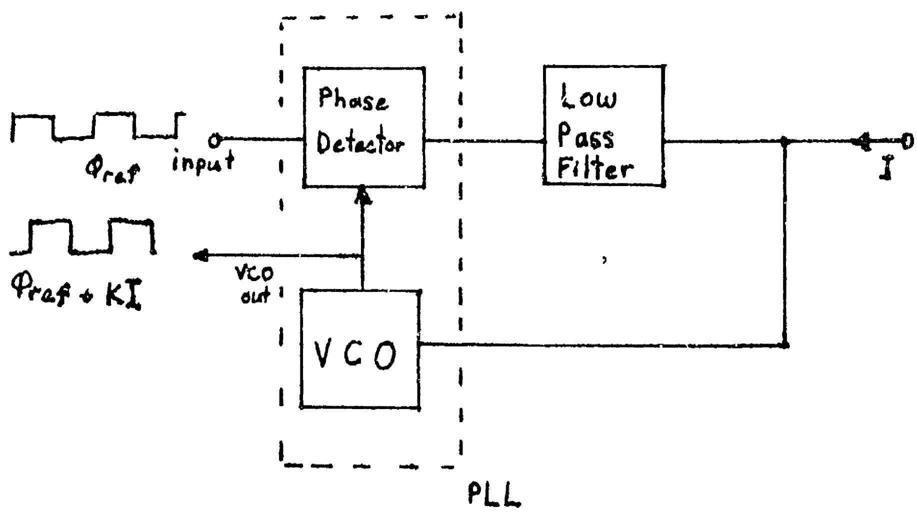
Phase
Detector
Low
Pass
Filter
VCO
PLL
input
VCO
out
φ_{ref}
$\varphi_{ref} + KI$
I

figure 11

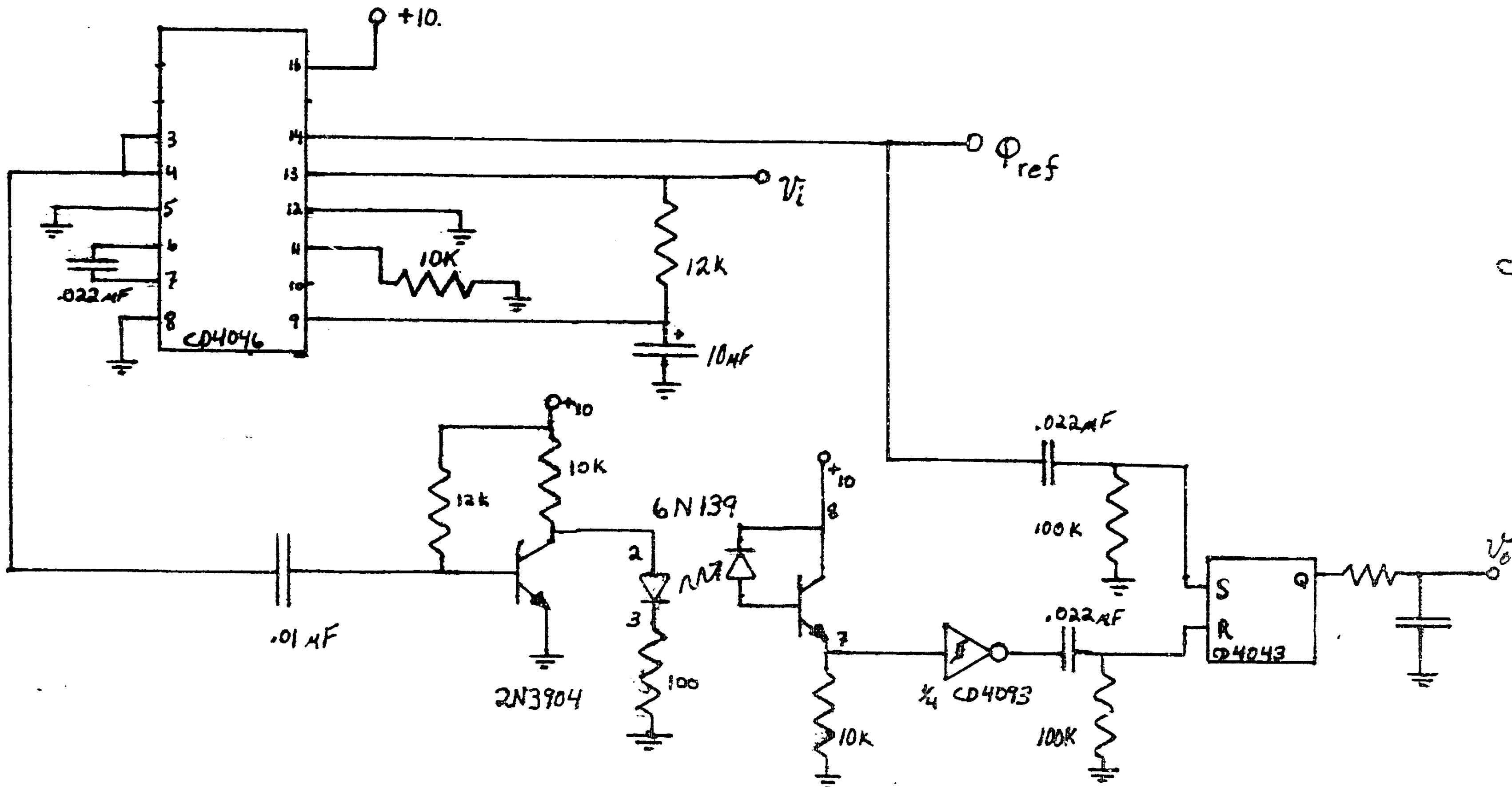
+10.
CD4046
3
4
5
6
7
8
16
14
13
12
11
10
9
.022μF
10K
12K
10μF
Φref
Vi
+10
10K
12k
6N139
2
3
100
.01μF
2N3904
+10
8
7
10K
¼ CD4093
.022μF
100K
.022μF
100K
S
R
Q
CD4043
Vo

figure 13

COMPARATIVE CHART FOR THE THREE ISOLATION CIRCUITS

	AM	FM	Phase
Power Required	less than 12 mW	25 mW	30 mW
linearity	excellent	excellent	good
Physical size	very small	limited to size of several DIP devices	
number of signal paths	1	1	2 (reference required)

Figure 14

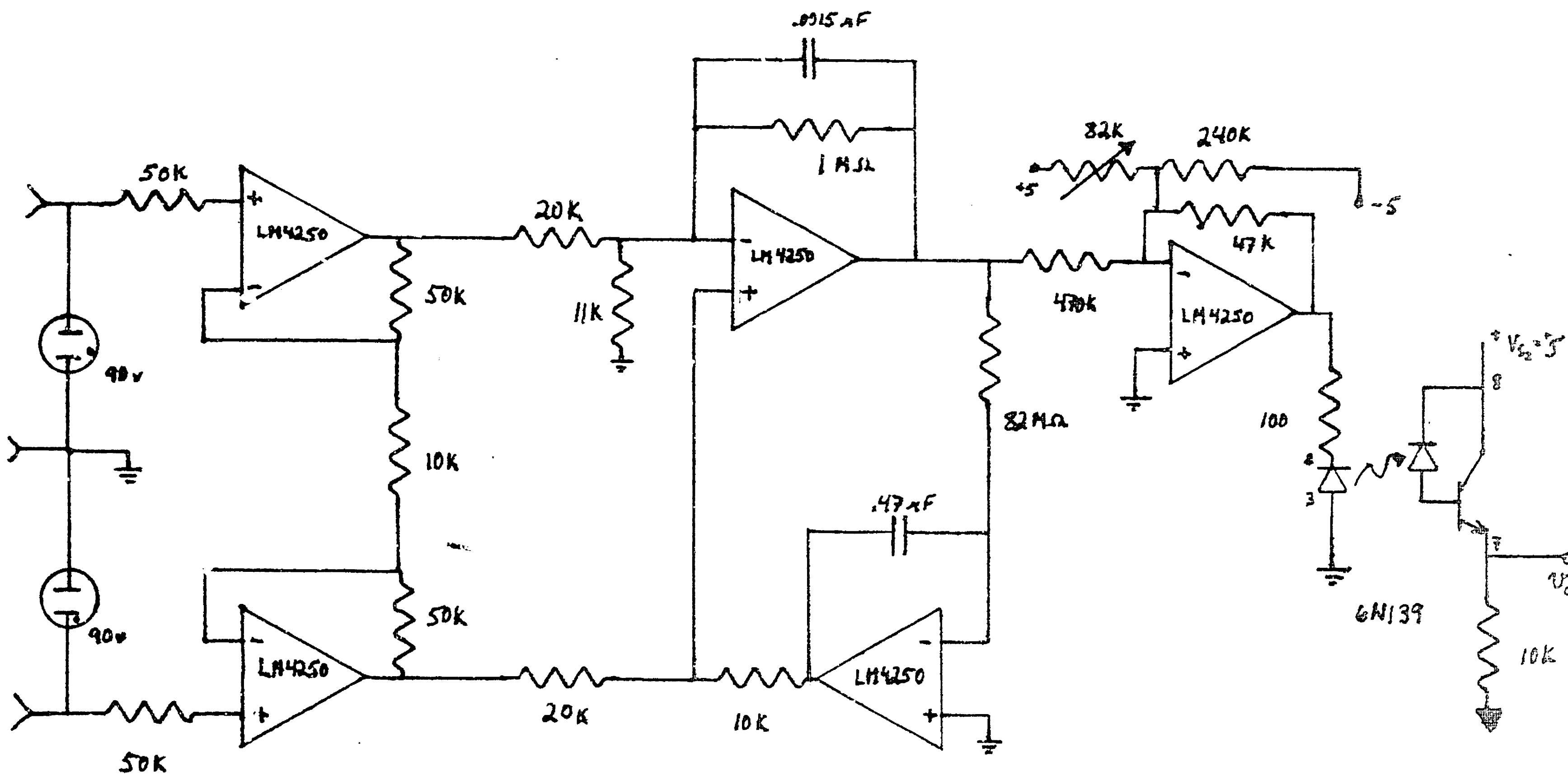
50K
LM4250
20K
.0015 μF
1 MΩ
LM4250
82K
240K
+5
-5
47K
LM4250
90v
50K
11K
470K
10K
82 MΩ
+ V_{S_2} = 5
100
.47 μF
6N139
V_o
90v
50K
LM4250
LM4250
10K
50K
20K
10K

figure 15

Table 1

6N139 LED V-I characteristics

V_d (volts)	$I_d = I_F$ (mA)
0	0
1.24	.030
1.26	.04
1.29	.06
1.30	.08
1.32	.115
1.34	.16
1.4	.5
1.46	1.0
1.50	5.0
1.54	10.

Table 2

6N139 LED diode approximation for V-I

using $I_d = (7.5 \times 10^{-12})\, e^{(17.8)(V_d)}$

V_d (volts)	measured or extrapolated I_d (mA)	approximation I_d (mA)
1.2	.014	.014
1.24	.030	.028
1.26	.04	.040
1.29	.06	.067
1.30	.08	.080
1.32	.115	.115
1.34	.16	.164
1.4	.5	.48

Table 3

AM test circuit

V_i (mV RMS)	V_0 (mV RMS)
f= 100 Hz	
170.60	117.15
130.93	89.90
76.27	52.48
55.70	38.40
36.06	25.02
23.25	16.30
13.64	10.00
.36	3.40
f= 10 Hz	
143.0	104.7
109.	80.5
74.	54.
8.05	7.0
.35	3.7

Table 4

FM circuit data at DC

V_i (volts)	V_o (volts)
3.805	5.507
4.445	5.407
4.520	5.398
4.871	5.328
5.441	5.236
5.799	5.157
6.010	5.109
6.516	4.953
6.798	4.867
7.137	4.590
7.729	3.784

Table 5

Phase modulation data

V_i (volts RMS)	V_o (volts RMS) at f= 30 Hz
.3180	.6687
.3347	.8146
.3584	1.0119
.3671	1.0808
.3825	1.2354
.3315	.7887
.3575	.9960